

## ORIGINAL ARTICLE

# Compensatory Actions of Ldb Adaptor Proteins During Corticospinal Motor Neuron Differentiation

Dino P. Leone<sup>1</sup>, Georgia Panagiotakos<sup>2</sup>, Whitney E. Heavner<sup>1</sup>, Pushkar Joshi<sup>1</sup>, Yangu Zhao<sup>3</sup>, Heiner Westphal<sup>3</sup> and Susan K. McConnell<sup>1</sup>

<sup>1</sup>Department of Biology, Stanford University, Stanford, CA, USA, <sup>2</sup>Department of Biochemistry and Biophysics, The Ely and Edythe Broad Center of Regeneration Medicine and Stem Cell Research, University of California, San Francisco, CA, USA, and <sup>3</sup>Laboratory of Mammalian Genes and Development, Program in Genomics of Development, Eunice Kennedy Shriver National Institute of Child Health and Human Development, National Institutes of Health, Bethesda, MD, USA

Address correspondence to Susan K. McConnell. Email: suemcc@stanford.edu

## Abstract

Although many genes that specify neocortical projection neuron subtypes have been identified, the downstream effectors that control differentiation of those subtypes remain largely unknown. Here, we demonstrate that the LIM domain-binding proteins *Ldb1* and *Ldb2* exhibit dynamic and inversely correlated expression patterns during cerebral cortical development. *Ldb1*-deficient brains display severe defects in proliferation and changes in regionalization, phenotypes resembling those of *Lhx* mutants. *Ldb2*-deficient brains, on the other hand, exhibit striking phenotypes affecting layer 5 pyramidal neurons: Immature neurons have an impaired capacity to segregate into mature callosal and subcerebral projection neurons. The analysis of *Ldb2* single-mutant mice reveals a compensatory role of *Ldb1* for *Ldb2* during corticospinal motor neuron (CSMN) differentiation. Animals lacking both *Ldb1* and *Ldb2* uncover the requirement for *Ldb2* during CSMN differentiation, manifested as incomplete CSMN differentiation, and ultimately leading to a failure of the corticospinal tract.

**Key words:** brain development, corticospinal motor neurons, differentiation, Ldb

## Introduction

The identification of key factors that specify neocortical pyramidal neuron subtypes, such as *Satb2* (callosal; [Alcamo et al. 2008](#); [Britanova et al. 2008](#); [Leone et al. 2015](#)), *Tbr1* (layer 6 corticothalamic; [Hevner et al. 2001](#); [Han et al. 2011](#); [McKenna et al. 2011](#)), and *Fezf2* (layer 5 subcerebral; [Chen B et al. 2005](#); [Chen JG et al. 2005](#); [Molyneaux et al. 2005](#); [Shim et al. 2012](#)), has dramatically increased our understanding of initial cell fate specification in the neocortex. However, it has become clear that initial specification is only the first step in a cascade of events that culminates in the manifestation of appropriate subtype-specific identity. The downstream regulatory mechanisms that control the differentiation of neuronal subtypes remain poorly understood. Here, we focus on corticospinal motor neurons (CSMNs)

in layer 5B of sensorimotor areas, which control fine and precise voluntary movements. They provide a valuable model to study differentiation due to their thorough molecular characterization ([Arlotta et al. 2005](#); [Chen B et al. 2005](#); [Chen JG et al. 2005](#); [Molyneaux et al. 2005](#); [Shim et al. 2012](#)) and distinct axonal trajectory to the spinal cord via the corticospinal tract (CST; [Jones et al. 1982](#)). While genes such as *Sox5* ([Kwan et al. 2008](#)), *Ctip2* ([Arlotta et al. 2005](#)), *CoupTF1* ([Tomassy et al. 2010](#)), and *Bhlhb5* ([Joshi et al. 2008](#)) have been implicated in some aspects of CSMN differentiation, the genetic program that governs their maturation remains poorly understood. CSMNs are susceptible to damage and death in neurological conditions such as stroke, spinal cord injury, and neurodegenerative disorders such as amyotrophic lateral sclerosis. A comprehensive elucidation of the genetic cascade that drives CSMN specification and differentiation will thus support

efforts to design optimal cell replacement therapies for the treatment of these debilitating conditions.

In this study, we describe the roles of Ldb adaptor proteins (LIM domain-binding proteins; also called Clim and NLI), which bind to LIM domains of LIM homeodomain (LIM-HD) and LIM-only (Lmo) proteins (Agulnick et al. 1996; Jurata et al. 1996; Bach et al. 1997). Ldb proteins have an intrinsic capability for dimerization, which allows LIM-HD proteins to interact with other LIM-HD proteins and/or regulatory proteins such as Otx, GATA, and bHLH (Wadman et al. 1994, 1997; Bach et al. 1997; Jurata and Gill 1997; Visvader et al. 1997; Breen et al. 1998; Meier et al. 2006). This capacity for dimerization enables LIM-HD proteins to form both homomeric and heteromeric complexes [reviewed in Matthews and Visvader (2003)].

There are 2 *Ldb* family members in vertebrates, 4 in zebrafish, and 1 each in *Caenorhabditis elegans* and *Drosophila melanogaster* [reviewed in Matthews and Visvader (2003)]. During cortical development, Ldb proteins may interact with the Lmo proteins Lmo3 and Lmo4, which are expressed in the developing cortex as early as E9.5 (Kenny et al. 1998; Sugihara et al. 1998; Bulchand et al. 2003). A germline deletion of *Lmo4* leads to defects in neural tube closure (Tse et al. 2004; Lee et al. 2005) and perinatal lethality, while a neocortex-specific knockout of *Lmo4* alters the formation of somatosensory barrel fields (Huang et al. 2009). A more recent study has shown that *Lmo4* forms a complex with Ngn2 and Ldb1 that co-activates Ngn2-dependent transcription (Asprey et al. 2011). A second major group of interaction partners for Ldb proteins is the LIM-HD family of Lhx proteins. *Lhx5*-deficient animals show disruptions of hippocampal development (Zhao et al. 1999), and *Lhx1/Lhx5* compound mutants show defects in Purkinje cell differentiation (Zhao et al. 2007). *Lhx2* plays several important roles during corticogenesis: The deletion of *Lhx2* results in neocortex hypoplasia and aplasia of the hippocampal anlagen (Porter et al. 1997), while *Lhx2* also functions as a cortical selector gene that specifies the neuroepithelium to adopt a cortical fate (Mangale et al. 2008). In addition, *Lhx2* specifies the regional fate of telencephalic neurons (Chou et al. 2009). Collectively, these studies suggest that Lhx and Lmo family members play varied and distinct roles during brain development.

To explore the role of Ldb proteins in cortical development, we took advantage of a conditional allele of *Ldb1* (Zhao et al. 2007), which we combined with *Emx1-Cre* to limit recombination to the dorsal neocortex (Gorski et al. 2002). Using *Emx1-Cre* allowed us to bypass both the lethality of the *Ldb1* germline null allele (Mukhopadhyay et al. 2003) and the early selector function of *Lhx2* (Mangale et al. 2008). To address the possibility that Ldb1 and Ldb2 play redundant roles during cortical development, we also analyzed *Ldb2* mutants and mice lacking both *Ldb1* and *Ldb2*.

Our studies reveal that *Ldb2* is upregulated specifically in layer 5 during development of the cerebral cortex. *Ldb1* exhibits an inversely correlated expression pattern: As cortical development proceeds, its early widespread expression in the cortical plate is progressively excluded from layer 5, concomitant with the acquisition of *Ldb2* expression. *Ldb1*-deficient mutants show a complex phenotype that includes proliferation defects and a fate change of lateral neocortex into piriform cortex, reminiscent of *Lhx2* null mutants (Chou et al. 2009). *Ldb2*-deficient mice display a normal CST, but layer 5 neurons show a dramatic compensatory upregulation of *Ldb1* and fail to properly segregate into callosal projection neurons (CPNs) and subcerebral projection neurons (SCPns). The analysis of compound nulls reveals incomplete molecular differentiation of CSMNs and a failure of the CST at the pyramidal decussation.

## Materials and Methods

### Generation of *Ldb2* Germline Null Allele

An FRT-neo cassette was cloned into the *AspI* sites of an 8.1-kb genomic *Ldb2* fragment (see Supplementary Fig. 1B). The *Ldb2*-Neo fragment was excised using *ClaI* and *SmaI*, and then cloned into a pDTA vector using *ClaI* and *EcoRV* sites. PCR-positive embryonic stem cell clones were screened using Southern blots, a 5' probe (3.3 kb) was used on *AspI*-cut DNA, and a 3' probe (1.4 kb) was used on *XbaI*-cut DNA.

### Animals

Mice hemizygous for either Nestin-Cre or Emx-Cre, carrying *Ldb1*<sup>lox/wt</sup> and *Ldb2*<sup>0/wt</sup>, were crossed with *Ldb1*<sup>lox/lox</sup>; *Ldb2*<sup>0/0</sup> mice to obtain mutant and control littermates. For some experiments, animals were also hemizygous for either Z/EG or Golli- $\tau$ -EGFP. See Supplementary Methods for genotyping. The morning of the vaginal plug observed was considered as E0.5. For proliferation assays, pregnant females were injected with 1 mg BrdU (in PBS) 2 h prior to analysis. In utero electroporations were performed as previously described (Ohtsuka et al. 2001). Briefly, a plasmid-expressing Cre recombinase, driven by a CAG promoter, was in utero electroporated into the ventricles of E12.5 embryos.

### Histology, Immunocytochemistry, Antibodies, and In Situ Hybridization

Standard methods of immunohistochemistry were used for immunocytochemical stainings. Animals were perfused with 4% paraformaldehyde in PBS, cryoprotected in 30% sucrose in PBS, and either embedded in OCT tissue-tek for cryosectioning or directly cut on a sliding microtome at 70–100  $\mu$ m. For BrdU stainings, sections were immersed in 10 mM citric acid (pH 6.0) at 94 °C for 25 min before proceeding with standard immunohistochemistry. In situ hybridization was carried out as previously described (Frantz et al. 1994); see Supplementary Methods for the complete list of probes.

We used a rabbit-anti-Ldb1 antibody (gift of Dr Paul Love, National Institutes of Health), rat-anti-Ctip2 (Abcam), mouse-anti-Tuj1 (Covance), both mouse- and rabbit-anti-Satb2 (Abcam), rabbit-anti-Tbr2 (Abcam), rat-anti-BrdU (Accurate Chemical), rabbit-anti-Tbr1 (Abcam), goat-anti-Lhx2 (Santa Cruz Biotech), goat-anti-Lmo4 (Santa Cruz Biotech), both rabbit- and chicken-anti-GFP (Abcam), rat-anti-L1 (Millipore), and rabbit-anti-PCP $\gamma$  (Santa Cruz Biotech). Alexa Fluor-coupled secondary antibodies were used to detect primary antibodies.

Confocal images were acquired on a Zeiss LSM 510 meta confocal microscope, and epifluorescent images were acquired on a Nikon 80i microscope with a Hamamatsu Orca ER camera. Images were postprocessed using ImageJ and Adobe Photoshop CS3.

### Retrograde Tracings

For retrograde tracings from the cervical spinal cord, P28 animals were anesthetized with isoflurane and placed on a stereotactic set-up for surgery. Cervical spinal cord was surgically exposed and 0.2–0.3  $\mu$ L of fluorescent-labeled latex beads (Lumafuor, Inc.) were injected into the ventral dorsal funiculus using a stereotactic injector (Stoelting). Animals were sacrificed 48–60 h after surgery to allow for transport of the beads.

## Results

### Ldb1 and Ldb2 Show Inversely Correlated Expression Patterns During Cortical Development

The Lim domain-binding protein Ldb2 (also known as Clim1 or NLI) is an excellent candidate for the study of CSMN differentiation. First, *Ldb2* is expressed in the neocortex (Bulchand et al. 2003) in a pattern that overlaps with *Fezf2*, which is required for CSMN fate specification (Chen B et al. 2005; Chen JG et al. 2005; Molyneaux et al. 2005). Second, *Ldb2* expression is abolished specifically in layer 5B of *Fezf2*<sup>-/-</sup> mice (Chen B et al. 2005; Molyneaux et al. 2005), implicating *Ldb2* as a potential downstream effector of *Fezf2* in the genesis of the CST. Third, there is a delay in the onset of *Ldb2* expression in layer 5 neurons, suggesting a role in differentiation but not in initial specification of CSMN identity: in a microarray screen for genes expressed differentially in newly postmitotic neurons between E12.5 and E16.5, *Ldb2* showed a dramatic increase in expression by E14.5, a time that correlates with the birth and migration of layer 5 neurons, with even more elevated expression by E16.5 (data not shown).

These results were corroborated by in situ hybridization: at E12.5, *Ldb2* expression is barely detectable in the neocortex (see Supplementary Fig. 1A and Bulchand et al. 2003). However, by E14.5, we detect a dramatic upregulation in layer 5B of the cortical plate (Fig. 1A) with robust expression at E16.5 (Fig. 1B) and P0 (Fig. 1C). Due to its restricted and delayed expression pattern in layer 5B, we hypothesized that *Ldb2* might be involved in maturation but not in initial specification of CSMNs. To investigate this possibility, we examined the status of the CST in P60 mice lacking *Ldb2* (see Supplementary Fig. 1B,C) by immunolabeling for protein kinase C  $\gamma$  (PKC $\gamma$ ), a specific marker for the CST (Mori et al. 1990). The analysis of cervical spinal cord cross-sections reveals an intact CST in *Ldb2* mutants (Fig. 1D') that is indistinguishable from controls (Fig. 1D).

The lack of CST aberrations in *Ldb2*-null mice prompted us to examine potential functional redundancy and compensation of *Ldb2* by its close family member *Ldb1* during CSMN differentiation. Strikingly, *Ldb1* is widely expressed across the cortical wall at E12.5 (Fig. 1E). At this age, newly generated neurons of layer 6 are migrating outward to populate the cortical plate.

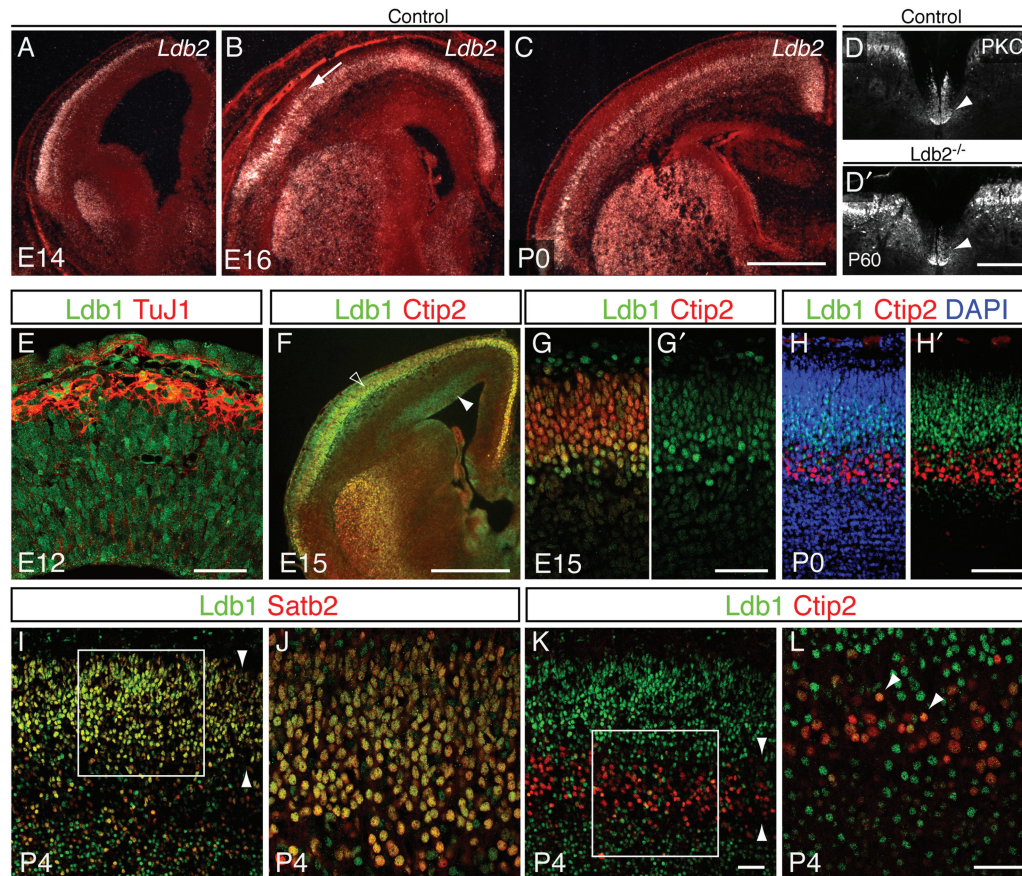


**Figure 1.** Inverse correlation of expression of *Ldb1* and *Ldb2* in layer 5 neurons. (A–C) In situ hybridization for *Ldb2*. High *Ldb2* expression is first detected in the cortical plate at E14 (A) and robust expression is seen in layer 5B at E16 (B; arrow) and P0 (C). The corticospinal tract, labeled by PKC $\gamma$  expression in the ventral dorsal funiculus (arrowheads in D and D'), is unaffected by loss of *Ldb2* (D') compared with controls (D). (E–L) Immunocytochemistry on coronal brain sections shows progressive exclusion of *Ldb1* protein (green in E–L) from layer 5 neurons during cortical development. (E) At E12, *Ldb1* is expressed by neurons of the cortical plate, labeled with TuJ1, and by progenitors lining the ventricular surface (arrowhead). (F) Low-power magnification shows *Ldb1* expression at E15 in the VZ (arrowhead) and partial overlap with *Ctip2* in the cortical plate (open arrowhead). (G and G') High-power confocal imaging reveals partial exclusion of *Ldb1* from *Ctip2*<sup>+</sup> neurons while some *Ctip2*<sup>+</sup> neurons still coexpress *Ldb1*. (H and H') At P0, *Ldb1* and *Ctip2* expression have segregated to a large extent. (I) By P4, *Ldb1* largely overlaps with *Satb2*. Arrowheads delineate upper layers 2–4. (J) High-power confocal imaging of boxed area in I shows virtually all *Satb2*<sup>+</sup> neurons coexpressing *Ldb1* (appearing yellow). (K) Doublestaining of *Ldb1* and *Ctip2* at P4 shows almost complete exclusion of *Ldb1* from *Ctip2*<sup>+</sup> layer 5 neurons (layer 5 delineated by arrowheads). (L) High-power confocal picture of boxed area in K confirms the absence of *Ldb1* in *Ctip2*<sup>+</sup> neurons, although a small fraction shows low levels of *Ldb1* (arrowheads). Scale bars: 500  $\mu$ m in (C) for (A–C); 300  $\mu$ m in (D') for (D,D'); 100  $\mu$ m in (E), 500  $\mu$ m in (F); 50  $\mu$ m in (G') for (G,G'); 100  $\mu$ m in (H') for (H,H'); 100  $\mu$ m in (K) for (I,K); 100  $\mu$ m in (L) for (J,L).

Immunocytochemical analyses reveal that *Ldb1* is expressed both by neural progenitors that line the apical surface and by differentiated neurons in the cortical plate, as revealed by counterstaining with TuJ1 (Fig. 1E). However, during mid-corticogenesis, at E15.5, *Ldb1* begins to become progressively excluded from layer 5B SCPNs: At E15.5, *Ldb1* shows partial coexpression with *Ctip2* (Fig. 1F), a transcription factor expressed by layer 5 SCPN (Arlotta et al. 2005, 2008), and hints of differential expression levels within layer 5 become obvious. While some *Ctip2*<sup>+</sup> layer 5 neurons strongly express *Ldb1*, the majority shows a reduced expression level (Fig. 1G,G'), suggesting a downregulation of *Ldb1* in *Ctip2*<sup>+</sup> SCPNs. Indeed, by P0, expressions of *Ctip2* and *Ldb1* are mostly exclusive: *Ldb1* is expressed by upper layer neurons and cells in layer 6 (Fig. 1H,H'). By postnatal day 4 (P4), when upper layer neurons have reached their final destination, *Ldb1* is coexpressed with *Satb2* (Fig. 1I,J), a marker for CPNs (Alcamo et al. 2008; Britanova et al. 2008; Leone et al. 2015), but is excluded from *Ctip2*<sup>+</sup> neurons in layer 5 (Fig. 1K,L). These data reveal that *Ldb2* and *Ldb1* display inversely correlated expression patterns that suggest a specific requirement for *Ldb2* in layer 5 SCPNs during differentiation.

### Loss of *Ldb1* Leads to Cortical Proliferation Defects

We generated a germline null allele of *Ldb2* by replacing its third exon, which encodes part of the essential Lim-binding domain, with a neomycin cassette, thus leading to a truncated, non-functional *Ldb2* allele (see Supplementary Fig. 1B,C and Methods). *Ldb2*-deficient animals (*Ldb2*-KO) do not display any obvious defects in the gross morphology of the brain (Fig. 2B). However, the cerebral hemispheres of *Emx1-Cre*<sup>+</sup>;*Ldb1*<sup>lox/lox</sup> mutants (*Ldb1*-KO) and *Emx1-Cre*<sup>+</sup>;*Ldb1*<sup>lox/lox</sup>;*Ldb2*<sup>-/-</sup> double knockouts (*Ldb1/2*-DKO) are strikingly smaller (Fig. 2C,D) than littermate controls (Fig. 2A), even though the mutants survive into adulthood, showing a statistically significant reduction in both anterior–posterior (Fig. 2E; a–p) and medio-lateral (Fig. 2E; med.-lat.) lengths. We reasoned that the size reduction in the cortical hemispheres could be due to defects in proliferation, differentiation, or cell survival.

To measure progenitor proliferation, we injected pregnant females with BrdU at E12.5, sacrificed embryos 2 h later, and processed brain sections for BrdU immunohistochemistry. Quantification revealed a small but statistically significant reduction in BrdU incorporation at E12.5 in *Ldb1*-KO compared with controls (Fig. 1N; 45.3 ± 0.3% vs. 49.8 ± 1.0%; *P* = 0.02) and in *Ldb1/2*-DKO compared with controls (Fig. 1N; 46.2 ± 1.2% vs. 49.8 ± 1.0%; *P* = 0.02). To investigate whether radial glia or intermediate progenitor proliferation is affected by the loss of *Ldb1/2*, we analyzed brains at E15.5 for BrdU incorporation after a 2-h pulse. Colabeling with antibodies against *Tbr2* allowed us to distinguish between radial glia progenitors (*Tbr2*<sup>-</sup>) and subventricular zone (SVZ) intermediate progenitors (*Tbr2*<sup>+</sup>; Englund et al. 2005). To determine the fraction of proliferating radial glia progenitors, we counted the number of BrdU<sup>+</sup>;*Tbr2*<sup>-</sup> cells between the apical ventricular surface and the dorsal border of the *Tbr2*<sup>+</sup> domain (Fig. 2E–H). In control mice, 31.9 ± 1.4% of *Tbr2*<sup>-</sup> cells were BrdU<sup>+</sup> (Fig. 2O; *n* = 3 animals per genotype). In *Ldb2*-KO animals, this fraction was 35.5 ± 0.1%, not significantly different from controls (*P* = 0.064). However, in *Ldb1*-KO and *Ldb1/2* DKO mice, the fraction of BrdU<sup>+</sup>;*Tbr2*<sup>-</sup> cells was reduced significantly to 20.5 ± 2.7% (*P* = 0.017) and 21.6 ± 0.5% (*P* = 0.005), respectively. These data demonstrate that *Ldb1* is an essential cofactor for proliferation in radial glia progenitors. No statistically significant difference was found between *Ldb1*-KO and *Ldb1/2*-DKO, suggesting that the loss of *Ldb2* in an *Ldb1*-KO background does not lead to a further defect in proliferation (*P* = 0.373).

The findings that both *Ldb1*-KO and *Ldb1/2*-DKO mice show significant deficits in proliferating radial glia imply that their proliferative output may be affected by the loss of *Ldb1*. To determine whether production of radial glia-derived SVZ progenitors is compromised, we examined the number of *Tbr2*<sup>+</sup> cells across the 4 genotypes at E15.5 (Fig. 2I–L). Both *Ldb1*-KO and *Ldb1/2* DKO mice showed obvious deficits in the number of *Tbr2*<sup>+</sup> cells (Fig. 2K,L, respectively). In controls, 36.9 ± 0.7% of cells between the ventricular surface and the dorsal border of the *Tbr2*<sup>+</sup> domain expressed *Tbr2* (Fig. 2P; *n* = 3 animals). In *Ldb2*-KO mice, 38.9 ± 0.4% of cells were *Tbr2*<sup>+</sup> (*P* = 0.035; *n* = 3 animals), a small increase. Strikingly, in *Ldb1*-KO and *Ldb1/2*-DKO mice, these fractions were reduced significantly to 23.6 ± 4.2% (*P* = 0.043) and 27.4 ± 2.2% (*P* = 0.020), respectively.

These findings suggest that a reduced proliferative output by ventricular cells in the absence of *Ldb1* does indeed compromise the generation of SVZ progenitors. To assess whether subsequent SVZ proliferation is affected, we counted the fraction of BrdU<sup>+</sup> cells among the *Tbr2*<sup>+</sup> progenitors following a 2-h pulse of BrdU. However, we did not find a statistically significant change in *Ldb1*-KO or *Ldb1/2*-DKO compared with controls (data not shown), suggesting that although the initial production of the SVZ pool is compromised in both mutants, the remaining population of SVZ progenitors proliferates normally.

*Ldb1* can bind to *Lmo4* and Neurogenin2 (*Ngn2*) in a protein complex that enhances the transcription of *Ngn2*-dependent targets such as *Tbr2* (Asprer et al. 2011). *Lmo4*, in turn, is expressed by SVZ progenitors at E15.5 (Huang et al. 2009). It is conceivable that the absence of *Ldb1* protein in *Ldb1*-KO and *Ldb1/2*-DKO mice disables the *Lmo4*/*Ngn2* complex and leads to a reduction in downstream gene activation, including that of *Tbr2*. However, our observations suggest that a requirement for *Ldb1* for *Tbr2* expression does not seem to be absolute, given that *Tbr2*<sup>+</sup> progenitors are not lost entirely in *Ldb1*-KO and *Ldb1/2*-DKO brains.

### Lack of Hippocampus and Defects in Regionalization in *Ldb1*-Deficient Brains

We next ascertained whether the production of specific cortical cell types in postnatal brains is affected by the loss of *Ldb1* and/or *Ldb2*. Immunocytochemical analysis at P4 for *Ctip2*, which is expressed by layer 5 neurons, and *Tbr1*, a T-box transcription factor expressed by layer 6 cells (Hevner et al. 2001), revealed no obvious gross defects in the formation of layers 5 and 6 in *Ldb2*-KO mice (Fig. 3B,F) compared with controls (Fig. 3A,E). Despite their smaller sizes, *Ldb1*-KO and *Ldb1/2*-DKO brains showed a correct overall organization of layers 5 and 6 (Fig. 3C,D, respectively). However, these lines exhibited a loss of the hippocampal formation (Fig. 3G,H, respectively), a result anticipated by previous reports that the *Ldb*-interacting proteins *Lhx5* (Zhao et al. 1999) and *Lhx2* (Porter et al. 1997) are required for hippocampal development. It is plausible that the absence of *Ldb1*, which normally functions as an adaptor protein for *Lhx* transcription factors, renders both of these Lim homeobox proteins non-functional, leading to a failure of hippocampal specification in *Ldb1*-deficient brains. In accordance with this hypothesis, we observed reduced expression of signaling molecules such as *Wnt5a* and *Bmp7*, which are required by hippocampal precursor cells, in *Ldb1*-KO brains at E12.5 (data not shown). *Lhx2* itself, which is expressed predominantly by neurons of layers 2–4 at P4, did not show any obvious changes in any of the mutants compared with controls (see Supplementary Fig. 3M–P), aside from a slight, qualitative reduction in expression which is likely due to the lower neuronal numbers in *Ldb1*-KO and *Ldb1/2*-DKO.

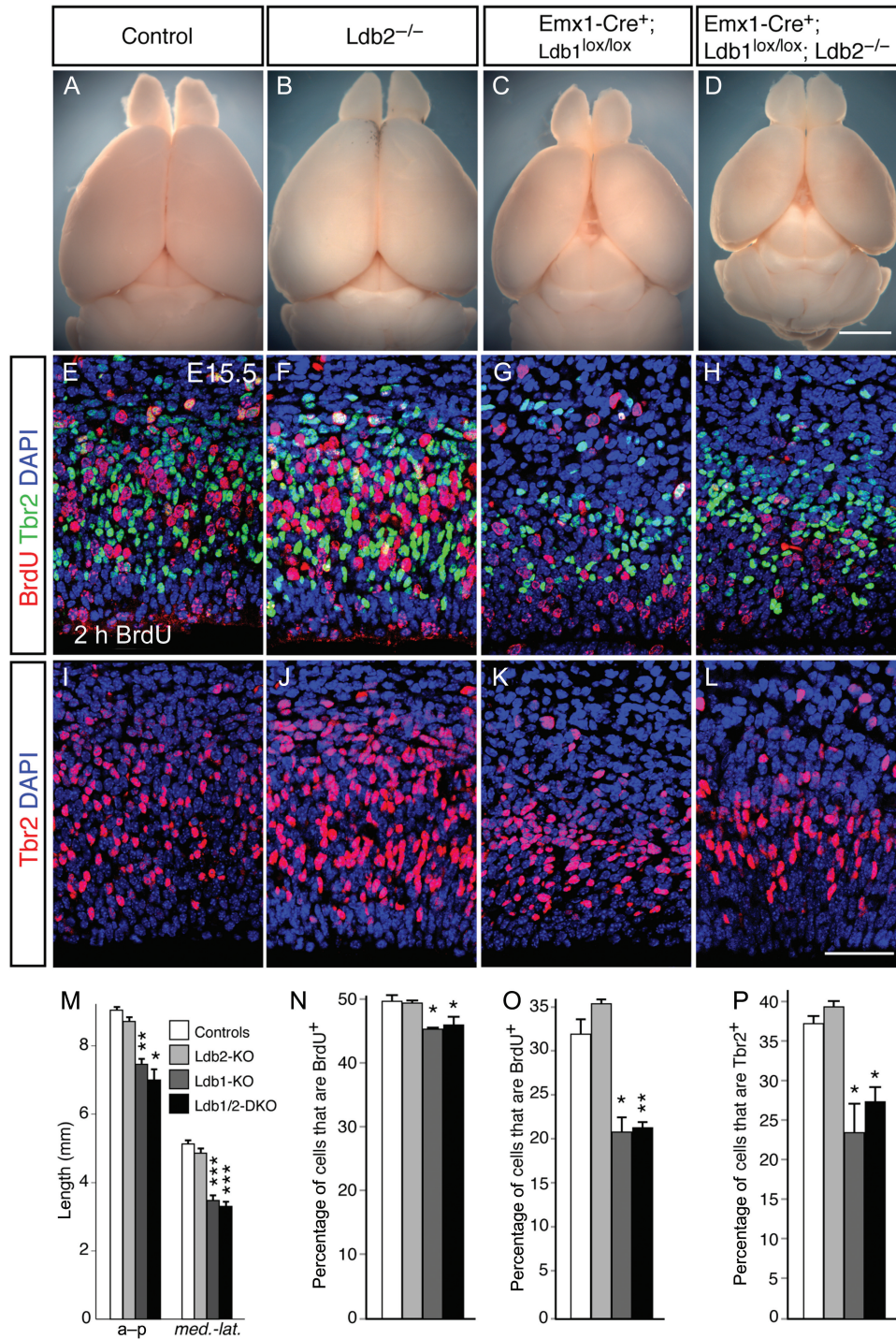


**Figure 2.** Proliferation defects in Ldb1-deficient mutants. (A–D) Whole mount brain preparations of 2-month-old animals show dramatic size reduction of cortical hemispheres in Ldb1-KO (C) and Ldb1/2-DKO (D) compared with controls (A) and Ldb2-KO (B). (E–L) Reduction in proliferative cells in Ldb1-KO and Ldb1/2-DKO. Two-hour BrdU pulse labeling at E15.5 reveals a dramatic reduction in the fraction of BrdU-labeled proliferating cells (red in E–H) in Ldb1-KO (G) and Ldb1/2-DKO (H) compared with control (E). No obvious change in BrdU incorporation was found in Ldb2-KO (F) compared with controls. (I–L) Immunocytochemical analysis for SVZ marker Tbr2 (red in I–L) shows striking reduction in the number of Tbr2<sup>+</sup> progenitors in Ldb1-KO (K) and Ldb1/2-DKO (L) compared with control (I). (M) Quantification of cortical size reductions shows a statistically significant reduction in both anterior–posterior (a–p) and medio-lateral dimensions (med.-lat.) in Ldb1-KO and Ldb1/2-DKO compared with controls and Ldb2-KO. (N) Quantification of BrdU incorporation after a 2-h pulse at E12.5 shows a significant reduction in BrdU incorporation at E12.5 in Ldb1-KO and Ldb1/2-DKO compared with controls. (O) Reduction in BrdU<sup>+</sup>;Tbr2<sup>-</sup> progenitor fraction in VZ at E15.5 shows a reduction in the percentage of BrdU<sup>+</sup> progenitor cells in both Ldb1-KO and Ldb1/2-DKO compared with controls. (P) Reduction in the percentage of Tbr2<sup>+</sup> intermediate progenitors at E15.5 in Ldb1-KO and Ldb1/2-DKO compared with controls. \*P ≤ 0.05; \*\*P ≤ 0.01; \*\*\*P ≤ 0.001. Scale bars: 2.5 mm in (D) for (A–D); 50 μm in (L) for (E–L).

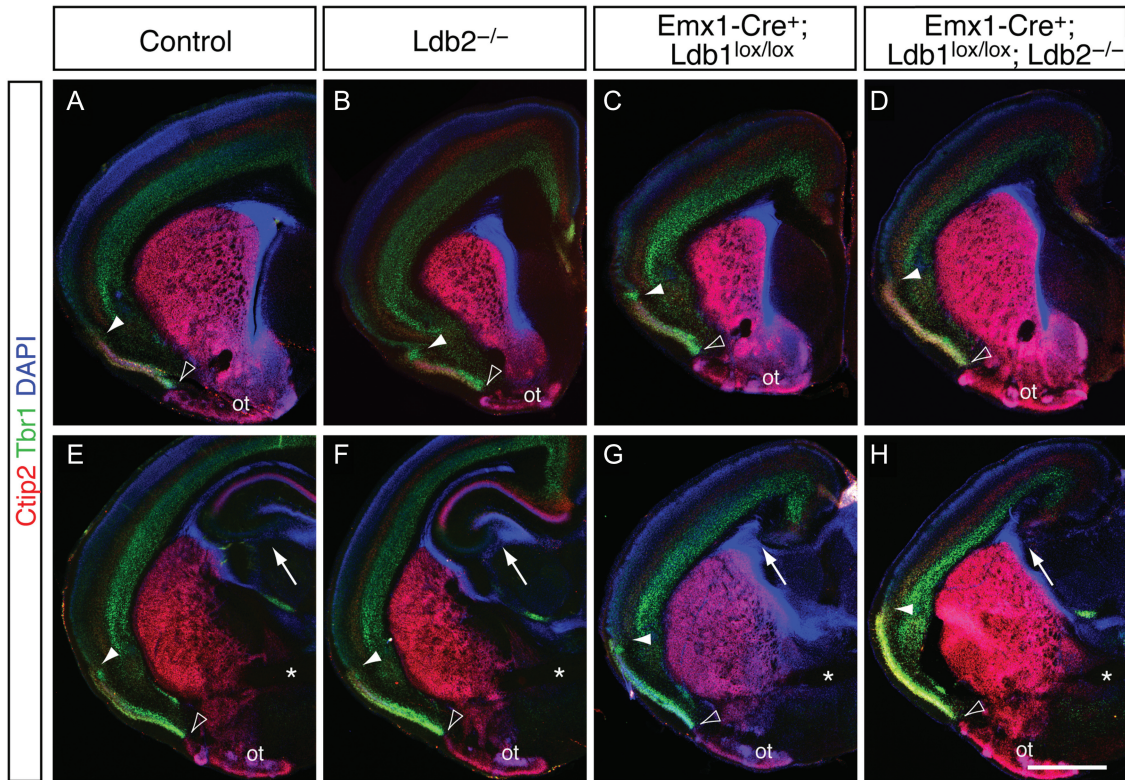


**Figure 3.** Lack of hippocampus and expansion of piriform cortex into lateral neocortex in *Ldb1*-deficient mutants. (A–H) Neocortical markers *Ctip2* (red in A–H) and *Tbr1* (green in A–H), which are expressed in layers 5 and 6, respectively, are also expressed in layer 2 of piriform cortex (demarcated by open and filled arrowheads), and *Ctip2* is robustly detected in the olfactory tubercle (ot). (A–D) Neocortical organization appears largely intact in *Ldb* mutants (B–D), but piriform cortex is expanded into lateral neocortex in *Ldb1*-KO (C) and *Ldb1/2*-DKO (D) compared with controls (A) and *Ldb2*-KO (B). Open arrowheads demarcate the ventral boundary of the piriform cortex, bordering the olfactory tubercle. Filled arrowheads indicate the dorsal/lateral boundary of the piriform cortex. (E–H) Sections at more posterior level show a similar expansion of piriform cortex in *Ldb1*-KO (G) and *Ldb1/2*-DKO (H) dramatically extends into the lateral neocortex. The hippocampus in both *Ldb1*-KO and *Ldb1/2*-DKO (arrows in G,H) is absent compared with controls and *Ldb2*-KO (arrows in E,F). Posterior sections in E–H were matched using the anterior commissure (asterisks in E–H) as a landmark. Scale bars: 1.3 mm in (H) for (A–H).

Prior studies showed that the neocortex-specific deletion of *Lhx2* leads to a fate conversion of neocortex into three-layered piriform cortex (Chou et al. 2009). The interaction of *Ldb* and *Lhx* proteins in this process generates the prediction that *Ldb1*-deficient brains should phenocopy this transformation. Indeed, the piriform cortex of mice lacking *Ldb1* expands into lateral neocortex, reminiscent of *Lhx2* knockout mice. In controls, piriform cortex, which borders the lateral neocortex at the rhinal fissure, is marked by strong immunoreactivity against *Ctip2* and *Tbr1* in layer 2, and the olfactory tubercle (Fig. 3A,E; Chou et al. 2009). While the piriform cortex of *Ldb2*-KO mice appears similar to controls (Fig. 3B,F), the markers expand into the lateral neocortex in *Ldb1*-KO mice (Fig. 3C,G) and in *Ldb1/2*-DKO brains (Fig. 3D,H). Fluorescent in situ hybridization for the piriform cortex-specific markers *Liprin  $\beta$ 1* (*Ppflbp1*) and *Slc6a7* confirmed these findings: Both markers, which are normally not detected in the dorsal neocortex, are ectopically upregulated in the *Ldb1*-KO neocortex. High-power confocal microscopic analysis of motor cortex allowed us to perform colocalization with *Satb2*, revealing that control brains express no *Liprin  $\beta$ 1* (see Supplementary Fig. 2A,A') in motor cortex, but *Ldb1*-KO mice show a striking expression of *Liprin  $\beta$ 1* (see Supplementary Fig. 2B,B'). *Slc6a7* is detected at low levels in control motor cortex (see Supplementary Fig. 2C,C'), but is robustly upregulated in *Ldb1*-KO brains (see Supplementary Fig. 2D,D'). The vast majority of *Liprin  $\beta$ 1*<sup>+</sup> cells do not coexpress *Satb2*, suggesting that the *Ldb1*-deficient motor cortex

houses 2 discrete cell populations—one piriform, the other neocortical—that are intermingled and coexist within a regionally hybrid area.

### Compensatory Upregulation of *Ldb1* in *Ldb2*<sup>-/-</sup> *Ctip2*<sup>+</sup> Layer 5 Neurons

The progressive exclusion of *Ldb1* from *Ctip2*<sup>+</sup> layer 5 neurons is concomitant with the emerging expression of *Ldb2* and is consistent with the idea that *Ldb2* might repress *Ldb1* expression in CSMNs. We thus hypothesized that the loss of *Ldb2* results in the ectopic expression of *Ldb1* in CSMNs, which can then compensate for *Ldb2* function in CSMN differentiation. To test this hypothesis, we first assessed P4 coronal sections for *Ldb1* expression. Low-power magnification reveals a striking upregulation of *Ldb1* in layer 5 of *Ldb2*-KO (Fig. 4B) compared with controls (Fig. 4A). Both *Ldb1*-KO and *Ldb1/2*-DKO (Fig. 4C,D) show *Emx1*-Cre-dependent loss of *Ldb1* in the neocortex, while striatal expression is maintained. *Ldb2* expression, on the other hand, is abolished in both *Ldb2*-KO and *Ldb1/2*-DKO (Fig. 4F,H) compared with controls (Fig. 4E), but appears unchanged in *Ldb1*-KO (Fig. 4G), suggesting that *Ldb2* cannot compensate for the loss of *Ldb1*. To further investigate the compensatory upregulation of *Ldb1* in *Ldb2* mutants, we performed high-power confocal microscopy for *Ldb1* in *Ctip2*<sup>+</sup> layer 5B SCPN at P4. In controls, the vast majority of *Ctip2*<sup>+</sup> SCPN do not express *Ldb1* (Fig. 4I,I').

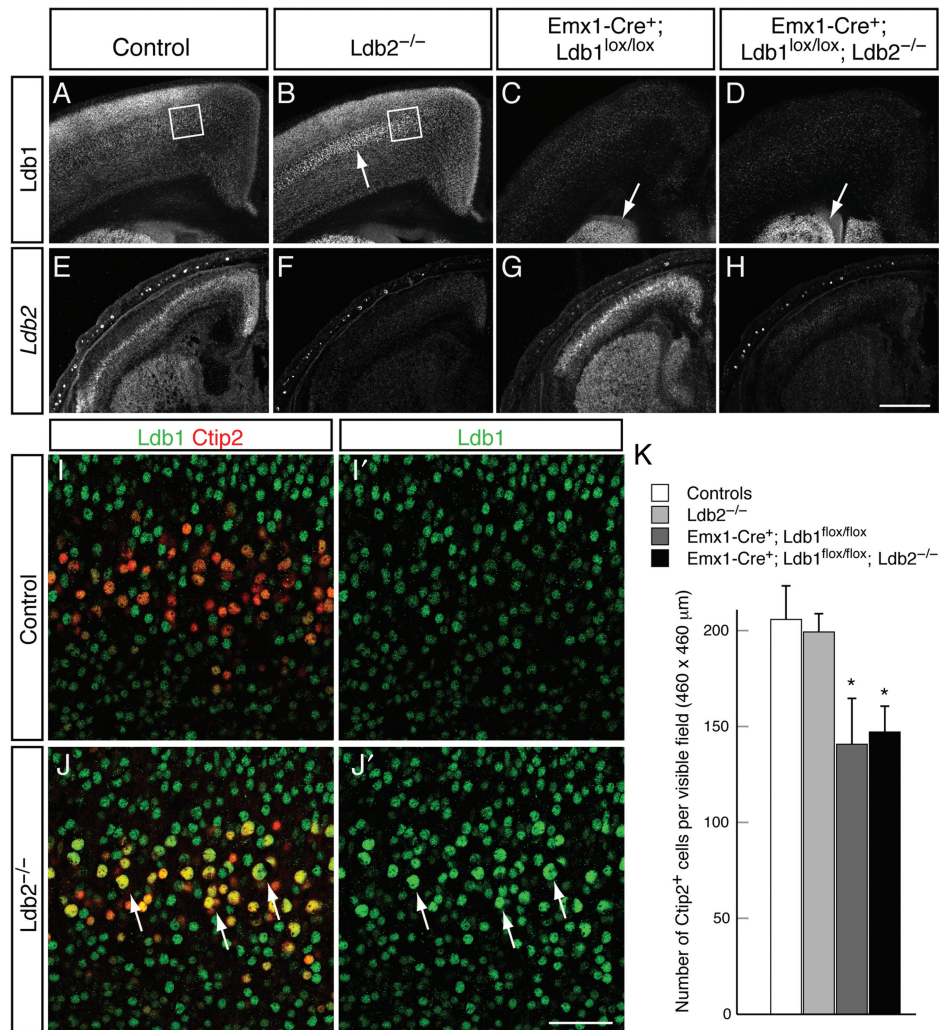


**Figure 4.** Compensatory upregulation of Ldb1 in Ldb2-deficient layer 5 neurons. (A–D) Immunocytochemical analysis of Ldb1 expression at P4 reveals striking upregulation of Ldb1 in layer 5 of Ldb2-KO neocortex (arrow in B) compared with control (A). Neocortex-specific loss of Ldb1 protein in pyramidal neurons of Ldb1-KO (C) and Ldb1/2-DKO (D). Remaining striatal expression of Ldb1 (arrows in C,D) confirms the specificity of the Emx1-Cre-dependent recombination. (E–H) In situ hybridization for *Ldb2* confirms loss of *Ldb2* mRNA in Ldb2-KO (F) and Ldb1/2-DKO (H), but no change in *Ldb2* expression in Ldb1-KO (G) compared with control (E). (I–J) High-power confocal analysis of layer 5 (boxed areas in A,B) confirms compensatory upregulation of Ldb1 (green in I–J) in Ldb2-deficient Ctip2<sup>+</sup> layer 5 neurons (red in J): In controls, Ctip2<sup>+</sup> layer 5 neurons do not express Ldb1 (I,I'). Strikingly, in Ldb2-KO, almost all Ctip2<sup>+</sup> neurons are coexpressing Ldb1 (yellow cells in J), including the large nucleated CSMN neurons (arrows in J,J'). A few Ctip2<sup>+</sup> neurons are detected that do not express Ldb1 (arrows in J; appearing red in J); however, all of them appear to have small nuclei. (K) Quantification of the absolute number of Ctip2<sup>+</sup> neurons across genotypes at P4. A statistically significant decrease in the number of Ctip2<sup>+</sup> neurons was found in Ldb1-KO and Ldb1/2-DKO compared with controls; however, Ldb1/2-DKO do not show any further reduction from Ldb1-KO. \* $P \leq 0.05$ . Scale bars: 500 μm in (H) for (A–H); 50 μm in (J') for (I–J').

However, in *Ldb2* mutants, an overwhelming majority of Ctip2<sup>+</sup> neurons were also Ldb1<sup>+</sup> (Fig. 4J,J'), suggesting that the loss of *Ldb2* leads to an ectopic, compensatory expression of Ldb1 in layer 5B SCPN.

Having shown that the loss of Ldb1 leads to proliferation defects, we wished to ascertain whether the absolute number of Ctip2<sup>+</sup> SCPNs was affected. Quantification of the number of Ctip2<sup>+</sup> neurons in the M1 motor area of 3 animals per genotype revealed no statistically significant changes in the number of Ctip2<sup>+</sup> neurons in Ldb2-KO mice compared with controls [Fig. 4K; 206 ± 17 cells per visible field (controls) vs. 199 ± 10 (Ldb2-KO;  $P = 0.38$ )]. In agreement with the proliferation defects observed (Fig. 2), both Ldb1-KO and Ldb1/2-DKO brains showed statistically significant decreases in the number of Ctip2<sup>+</sup> neurons [141 ± 24 (Ldb1-KO;  $P = 0.047$ ) and 147 ± 13 (Ldb1/2-DKO;  $P = 0.02$ )]. Importantly, we did not detect a further reduction in the numbers of Ctip2<sup>+</sup> neurons in Ldb1/2-DKO compared with

Ldb1-KO mice ( $P = 0.42$ ), suggesting that the additional loss of *Ldb2* in an Ldb1-KO background does not adversely affect survival of Ctip2<sup>+</sup> neurons.

### Impaired Segregation of Layer 5 Neurons in *Ldb2*<sup>-/-</sup> Mice

The upregulation of Ldb1 in Ldb2-KO layer 5B SCPNs motivated us to further examine this population of neurons. Recent work by Macklis and colleagues suggests that *Ldb2* and *Lmo4* expression can be used as markers to progressively demarcate layer 5 neurons as they differentiate toward either a SCPN or CPN fate, respectively (Azim et al. 2009). Although *Lmo4* and *Ldb2* are coexpressed by many layer 5 neurons at mid-cortigogenesis, the 2 markers segregate into 2 distinct populations with little overlap by P6. We hypothesized that if *Ldb2* is required for immature layer 5 neurons to acquire a SCPN identity, then loss of *Ldb2* might interfere with this process.

At P4, *Lmo4* is highly expressed in motor cortex of wild-type controls (Fig. 5A,E) within layer 5, delineated using *Ctip2* (in red, Fig. 5A–D), and in layer 6. In agreement with previous reports, *Lmo4* is also detected in the upper layers of somatosensory cortex (Bulchand et al. 2003; Huang et al. 2009). *Ldb1* is most strongly expressed by upper layer neurons of somatosensory cortex, and more weakly in motor and cingulate cortex (Figs 4A and 5A,E). In *Ldb2*-KO mice, we detected a subtle upregulation in *Lmo4* expression in layers 4 and 5 at low-power magnification (Fig. 5B,F); however, high-power confocal pictures from layer 5 of motor cortex revealed a dramatic increase in the coexpression of *Lmo4* with *Ctip2* (Fig. 5J) compared with controls

(Fig. 5I). Quantification revealed a statistically significant increase from  $6.9 \pm 1.1\%$  of *Ctip2*<sup>+</sup> cells coexpressing *Lmo4* (controls) to  $13.5 \pm 1.1\%$  (*Ldb2*-KO;  $P = 0.002$ ;  $n = 4$ ; Fig. 5M). Unexpectedly, we find striking changes in *Lmo4* expression in *Ldb1*-KO (Fig. 5C,G,K) and *Ldb1/2*-DKO mice (Fig. 5D,H,L): In *Ldb1*-KO brains, the motor/somatosensory boundary appears shifted laterally, and *Lmo4* expression is elevated diffusely over the cortical wall (Fig. 5C). In *Ldb1/2*-DKO mice, *Lmo4* expression is completely abolished across the neocortex (Fig. 5D,H,L; 0% *Lmo4/Ctip2* coexpression;  $P = 0.0001$ ;  $n = 4$ ), while striatal expression remains unaffected (Fig. 5H), due to the *Emx1*-Cre specificity to the neocortex.

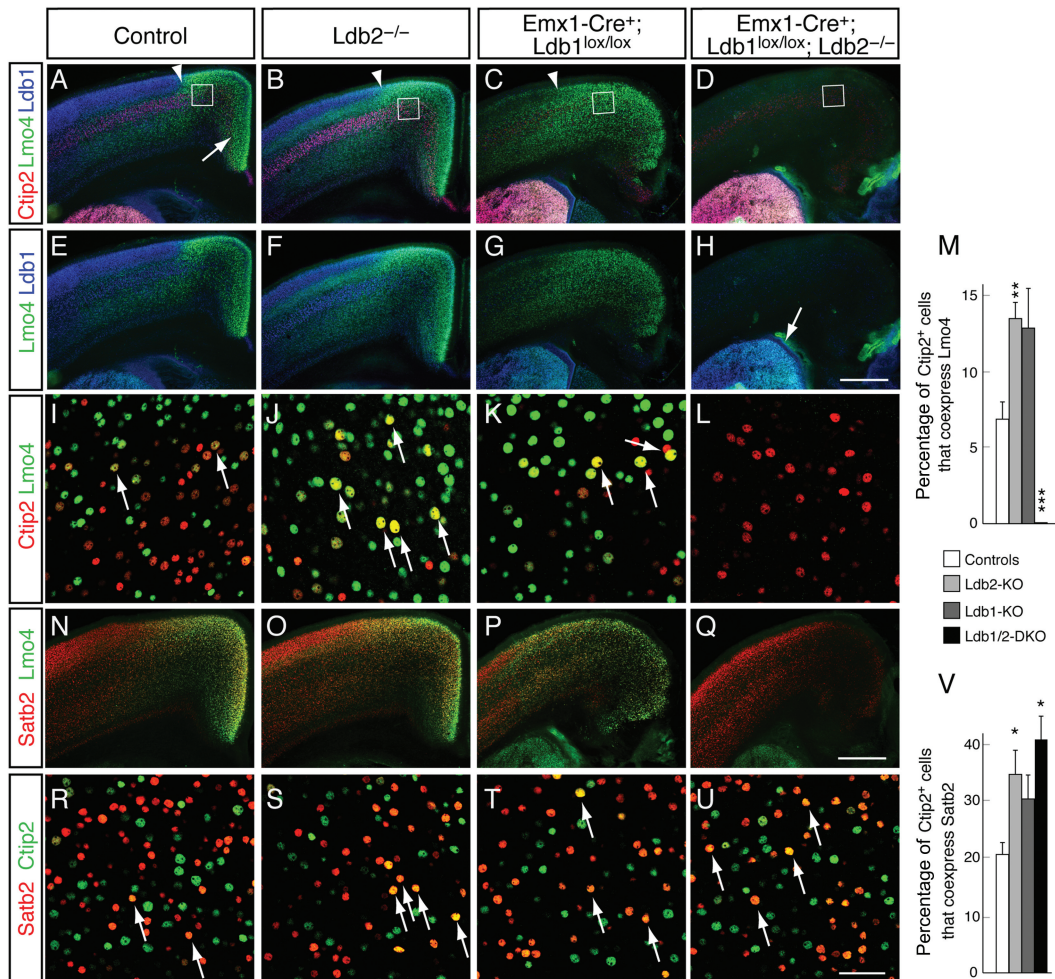


**Figure 5.** Impaired segregation of immature layer 5 neurons in the absence of *Ldb2*. (A–L) Immunocytochemical analysis shows striking *Ldb1/2*-dependent changes in *Lmo4* expression. *Lmo4* expression (green in A–L) is high in the cingulate cortex of controls (arrow in A), extends into motor cortex, and shows lower expression levels in layers 2/3 lateral to the motor/somatosensory boundary (arrowheads in A–C). *Lmo4* is also expressed by subsets of neurons of layers 4–6. *Ctip2* (red in A–D) was used to mark layer 5 neurons and *Ldb1* (blue in A–H) as a reference marker. Low-power magnification reveals a subtle upregulation of *Lmo4* in layers 4 and 5 of *Ldb2*-KO (B,F; arrows in J) compared with controls (A,E,I), while *Ldb1*-KO displays a striking ectopic upregulation of *Lmo4* across the cortical wall (C,G,K). *Lmo4* is completely lost in the neocortex of *Ldb1/2*-DKO (D,H,L), but striatal expression of both *Ldb1* and *Lmo4* (arrow in H) is maintained due to *Emx1*-Cre's neocortex specificity. (I–L) High-power confocal pictures of M1/M2 motor area of layer 5 (boxed in A–D) show colocalization between *Ctip2* (red in I–L) and *Lmo4* (green in I–L). The number of *Ctip2*<sup>+</sup>*Lmo4*<sup>+</sup> double-positive neurons (yellow in I–L) is increased in *Ldb2*-KO (J) and *Ldb1*-KO (K) compared with controls (I). Cortical *Lmo4* immunoreactivity is abolished in layer 5 of *Ldb1/2*-DKO (L). (M) Quantification of *Ctip2*/*Lmo4* coexpression reveals a statistically significant increase in coexpression in layer 5 neurons of *Ldb2*-KO compared with controls, and a dramatic loss in *Ldb1/2*-DKO. (N–U) Colabeling with a CPN marker *Satb2* (red in N–U) reveals partial overlap between *Lmo4* (green in N–Q) and *Satb2* in controls (N) and *Ldb2*-KO brains (O). *Satb2* expression is qualitatively reduced in *Ldb1*-KO (P) and *Ldb1/2*-DKO (Q), but *Satb2*<sup>+</sup> CPNs are present in *Ldb1/2*-DKO (Q), suggesting that these neurons have downregulated *Lmo4*. (R–U) Colabeling of *Satb2* and *Ctip2* shows very few *Ctip2*<sup>+</sup>*Satb2*<sup>+</sup> (yellow in R) double-positive neurons in layer 5 motor cortex of controls (arrows in R). An increased fraction of *Ctip2*<sup>+</sup> neurons coexpress *Satb2* in *Ldb2*-KO (arrows in S) and *Ldb1*-KO (T). A further increase in *Ctip2*<sup>+</sup>*Satb2*<sup>+</sup> double-positive layer 5 neurons (arrows in U) is found in motor cortex of *Ldb1/2*-DKO (U). (V) Quantification of *Ctip2*/*Satb2* coexpression shows statistically significant increases in the fraction of double-positive layer 5 neurons in *Ldb2*-KO and *Ldb1/2*-DKO compared with controls. \* $P \leq 0.05$ ; \*\* $P \leq 0.01$ ; \*\*\* $P \leq 0.001$ . Scale bars: 500  $\mu\text{m}$  in (H) for (A–H) and in (Q) for (N–Q); 50  $\mu\text{m}$  in (U) for (I–L) and (R–U).

The striking loss of cortical *Lmo4* expression in *Ldb1/2*-DKO mice could be the result of a downregulation of *Lmo4* (with the neurons themselves still present), or a loss of the population of *Lmo4*<sup>+</sup> neurons. To distinguish between these possibilities, we performed immunocytochemistry for the CPN marker *Satb2*. The analysis of control (Fig. 5N) and *Ldb2*-KO mice (Fig. 5O) revealed partial overlap between *Satb2* and *Lmo4*, and a qualitative reduction in *Satb2* immunoreactivity in *Ldb1*-KO brains (Fig. 5P). Given the proliferation defects seen in *Ldb1* mutants, the latter is likely due to a global reduction in the neuronal numbers (Fig. 2). *Ldb1/2*-DKO mice showed no further reduction in *Satb2* expression (Fig. 5Q), suggesting that *Satb2*<sup>+</sup> neurons are still present—albeit at reduced numbers—but have indeed downregulated *Lmo4*.

To further investigate the failure in segregation of layer 5 neuronal subtypes, we analyzed high-power confocal pictures for colocalization of *Satb2* and *Ctip2*. We hypothesized that the impaired segregation should also manifest itself in an increase in *Satb2/Ctip2* colocalization in layer 5 motor cortex neurons. Quantification indeed revealed that in motor cortex of *Ldb2*-KO mice,  $34.5 \pm 4.6\%$  of *Ctip2*<sup>+</sup> cells coexpressed *Satb2*, compared with  $20.4 \pm 1.7\%$  in controls (Fig. 5R,V;  $n = 3$ ,  $P = 0.045$ ). *Ldb1*-KO mice showed a nonsignificant increase in coexpression to  $30.0 \pm 5.3\%$  (Fig. 5T,V;  $n = 3$ ,  $P = 0.192$ ). We found that  $41.1 \pm 5.1\%$  of *Ctip2*<sup>+</sup> cells coexpress *Satb2* in *Ldb1/2*-DKO animals (Fig. 5U, V;  $n = 3$ ,  $P = 0.018$ ), a statistically significant increase compared with controls. The fact that we did not observe a further increase in *Satb2/Ctip2* coexpression in *Ldb1/2*-DKO compared with *Ldb2*-KO mice ( $P = 0.393$ ) implies that the loss of *Ldb1* does not compound the segregation defect observed in *Ldb2*-KO mutants. Taken together, the data suggest that *Ldb2* is required by immature layer 5 neurons to segregate into CPNs and SCPNs, and that the upregulation of *Ldb1* in *Ldb2*-KO *Ctip2*<sup>+</sup> neurons fails to functionally compensate for the loss of *Ldb2*.

### Incomplete Differentiation of CSMNs in *Ldb1/2*-DKO Mutants

The results above show that loss of *Ldb2* impairs the early differentiation of layer 5 neurons, and suggests that it might affect CSMN differentiation and ultimately their ability to form cortical efferents. To further investigate the potential compensatory actions of ectopic *Ldb1* expression in *Ldb2*<sup>-/-</sup> mutants, we evaluated CSMN differentiation. Significantly, none of the single or compound mutants show changes in the expression of layer 5B SCPN-enriched transcription factors *Fezf2* (see Supplementary Fig. 3A–D) or *Ctip2* (see Supplementary Fig. 3E–H), confirming that *Ldb* proteins do not regulate initial specification or migration of layer 5B SCPN.

Despite appropriate initial specification and survival, CSMNs exhibit incomplete molecular differentiation in compound mutants. In situ hybridization on coronal P1 sections reveals a loss of the CSMN-enriched genes *Foxo1* (Fig. 6A–D'), *Foxp2* (Fig. 6E–H'), and *Diap3* (Fig. 6I–L') in *Ldb1/2*-DKO mice. Notably, *Foxp2*, which is also expressed by layer 6 neurons, is abolished in layer 5B motor cortex of *Ldb1/2*-DKO brains, while layer 6 expression is unaffected, in support with the idea that loss of *Ldb1/2* specifically affects layer 5 CSMN differentiation. Expression of *Igf1bp4*, which is normally upregulated during terminal CSMN differentiation, is also abrogated in *Ldb1/2*-DKO mice (Fig. 6M–P'). Similarly, *Lmo3*, one of the potential binding partners for *Ldb* proteins, shows robust expression in layer 5 cells of controls and *Ldb2*-KO mice (see Supplementary Fig. 3I,J') at E15.5; however, *Lmo3* expression is completely abolished in the neocortex of *Ldb1/2*-DKO brains (see Supplementary Fig. 3L,L'), similar to *Lmo4*. The loss of differentiation markers specifically in *Ldb1/2*-DKO mutants suggests that the compensatory upregulation of *Ldb1* in layer 5B SCPN masks a phenotype in *Ldb2* single mutants.

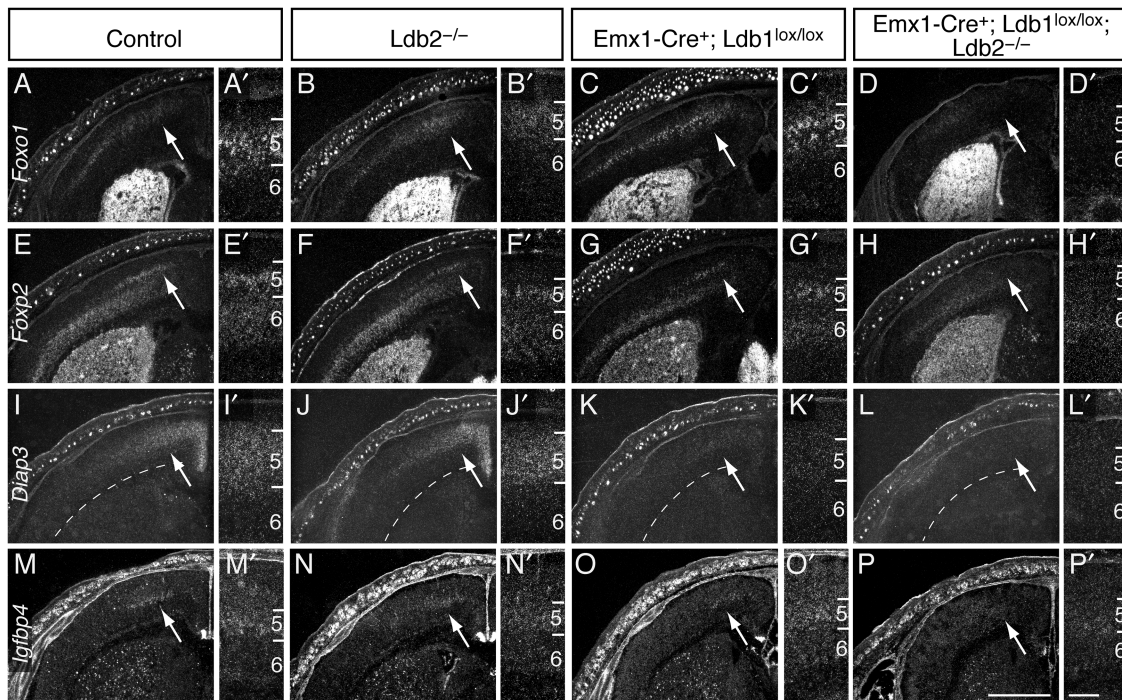


**Figure 6.** Incomplete molecular differentiation of CSMNs in *Ldb2*-deficient mutants. In situ hybridization on coronal P1 sections reveals loss of the differentiation markers *Foxo1* (A–D'), *Foxp2* (E–H'), *Diap3* (I–L'), and *Igf1bp4* (M–P') in layer 5 of motor cortex (arrows) in *Ldb1/2*-DKO mice. Note that layer 6 expression of *Foxp2* is not affected by the loss of *Ldb* genes, confirming the specific roles of *Ldb1/2* in layer 5 neurons. Scale bars: 1 mm in (P, main panels), 0.2 mm in (P', inset panels).

### CSMNs in *Ldb1/2*-DKO Mice Fail to Extend Their Axons Past the Pyramidal Decussation

The impairment in CSMN differentiation in *Ldb1/2*-DKO mutants prompted us to further investigate CSMN maturation. In particular, we wished to examine whether the differentiation defect would manifest itself at the level of axonal targeting to the spinal cord. We therefore analyzed CST formation in all 4 lines. To investigate subcortical projection pathways, we took advantage of the Z/EG Cre-dependent EGFP reporter line, which expresses EGFP upon Cre-mediated recombination (Novak et al. 2000). This system, combined with the *Emx1*-Cre allele, allowed us to label cortical efferent tracts such as the CST using EGFP.

At P4, EGFP<sup>+</sup> CST axons extend along the brainstem and cross into the dorsal funiculus of the spinal cord at the pyramidal decussation in control mice (Fig. 7A). The tract appears intact in both *Ldb2*-KO and *Ldb1*-KO brains (Fig. 7B,C, respectively); however, there is a striking failure of the CST at the pyramidal decussation in *Ldb1/2*-DKO mice (Fig. 7D). Among 8 *Ldb1/2*-DKO mutants examined, no EGFP<sup>+</sup> fibers were detected distal to the pyramidal decussation. High-power magnifications of the brainstem (boxed areas in Fig. 7A–D) revealed robust EGFP staining in the CST of controls (Fig. 7E) and *Ldb2*-KO mice (Fig. 7F). *Ldb1*-KO brains show a modest decrease in tract size and the tract appears defasciculated at this level (Fig. 7G), while *Ldb1/2*-DKO animals show a further reduction in tract size (Fig. 7H).

To exclude the possibility of a developmental delay, we analyzed cross-sections through the cervical spinal cord at P60 (Fig. 7I–L). In controls and single mutants, the CST is readily visualized by either PKC $\gamma$  or EGFP (Fig. 7I–K), but the tract is absent in *Ldb1/2*-DKO mice (Fig. 7L), consistent with the earlier failure of axons to progress beyond the pyramidal decussation in *Ldb1/2*-DKO mutants. Given the reduced number of Ctip2<sup>+</sup> layer 5 neurons in *Ldb1*-KO and *Ldb1/2*-DKO mice (Fig. 4K), a reduction in *Ldb1/2*-DKO tract size was expected compared with controls. However, since the number of Ctip2<sup>+</sup> neurons in *Ldb1/2*-DKO cortices is comparable with that in *Ldb1*-KO mice, neuronal numbers are unlikely to account for the further reduction in tract size. The absence of axons that extend past the pyramidal decussation in the *Ldb1/2*-DKO mice suggests severe defects at the pyramidal decussation.

To determine conclusively whether any CST axons in *Ldb1/2*-DKO mutants reach the spinal cord, we performed retrograde axonal tracing by injecting red fluorescent latex microspheres into the cervical ventral dorsal funiculus of 4-week-old mice. Animals were sacrificed 48 h after surgery to allow for transport of the tracer. Controls and single mutants revealed robust back-labeled CSMNs in layer 5B of the cortex (Fig. 7M–O), but only very few cortical neurons were back-labeled in *Ldb1/2*-DKO brains (Fig. 7P), confirming that the vast majority of CSMN axons fail to project beyond the pyramidal decussation into the spinal cord.

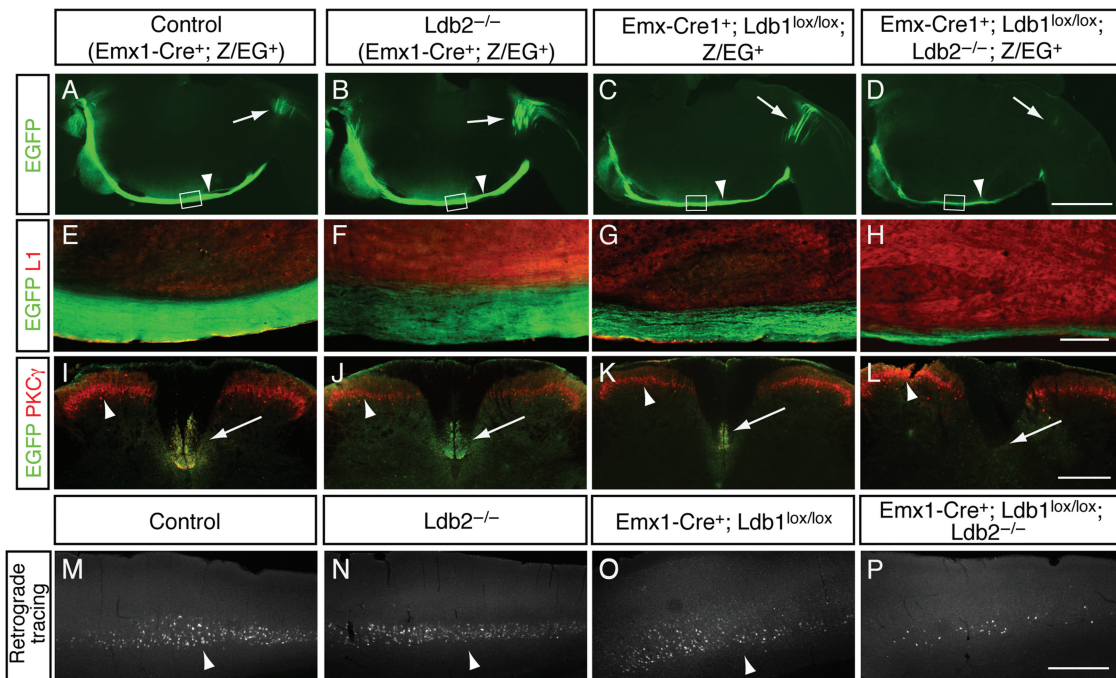


**Figure 7.** Failure of corticospinal tract in *Ldb1/2*-DKO mutants at the pyramidal decussation. (A–L) *Emx1*-Cre-dependent EGFP expression of the Z/EG reporter was used to specifically label neocortical pyramidal neurons and their efferent projections. (A–D) Sagittal brain sections of P4 animals reveal EGFP labeling in the CST along the brainstem (arrowheads in A–D), and the pyramidal decussation (arrows in A–D) of controls (A), *Ldb2*-KO (B), and *Ldb1*-KO (C). (D) In *Ldb1/2*-DKO, however, the tract fails at the decussation, and only very few crossing axons are detected (arrow in D). (E–H) High-power magnification of sagittal sections through the CST along the brainstem (boxed in A–D), counterstained with L1 (red in E–H), and reveals robust Z/EG-EGFP labeling in the CST of controls (E) and *Ldb2*-KO (F). A reduction in size of the tract is observed in *Ldb1*-KO (G), in agreement with the reduced number of Ctip2<sup>+</sup> neurons in *Ldb1*-KO (Fig. 4). A further reduction in tract size is observed in *Ldb1/2*-DKO (H). (I–L) Cross-sections through the cervical spinal cord of 4-week-old animals show the absence of CST in *Ldb1/2*-DKO. Immunocytochemical analysis for EGFP (green in I–L) and PKC $\gamma$  (red in I–L) reveals the CST in ventral dorsal funiculus of controls (arrow in I), *Ldb2*-KO (J), and *Ldb1*-KO (K), but the absence of the tract in *Ldb1/2*-DKO (arrow in L). PKC $\gamma$  also labels spinal cord interneurons (arrowheads in I–L). (M–P) Microinjection of fluorescent microspheres into the C2 level of the cervical spinal cord of 4-week-old animals shows retrogradely labeled CSMN in layer 5. Robust back-labeling in layer 5 is seen in controls (arrowhead in M) and *Ldb2*-KO (arrowhead in N). Fewer cells are found in layer 5 of *Ldb1*-KO (arrowhead in O), and only very few labeled neurons are seen in *Ldb1/2*-DKO (P). Scale bars: 1 mm in (D) for (A–D); 250  $\mu$ m in (H) for (E–H); 300  $\mu$ m in (L) for (I–L); 500  $\mu$ m in (P) for (M–P).

Previous reports have shown a role for *Lhx2* as a cortical selector gene (Mangale et al. 2008) and also as a fate determinant in that loss of *Lhx2* can lead to a respecification of cortical pyramidal neurons to piriform cortex identity (Chou et al. 2009). To investigate whether the observed failure of the CST in *Ldb1/2*-DKO mutants could be due to an early fate respecification, we deleted *Ldb1* specifically in the cortical plate by electroporation of a CAG-Cre plasmid at E12.5, bypassing the early specification period during which *Lhx2* is required, thereby ensuring *Lhx2* function for proper neocortical specification. Ai9 reporter-positive embryos carrying either *Ldb1<sup>lox/lox</sup>* or *Ldb1<sup>lox/wt</sup>* and either *Ldb2<sup>+/-</sup>* or *Ldb2<sup>-/-</sup>* were electroporated in utero with a Cre plasmid at E12.5 and analyzed at postnatal day 5 (P5) for CST formation, similar to the method described earlier. Cortical Cre electroporation leads to robust recombination of the Ai9 reporter allele, in turn labeling the CST in controls (see Supplementary Fig. 4A), *Ldb2*-KO (see Supplementary Fig. 4B), and *Ldb1*-KO mice (see Supplementary Fig. 4C). In Cre-electroporated *Ldb1/2* double mutants, however, the CST reaches the pyramidal decussation, but fails to project further caudally (see Supplementary Fig. 4D). The defect in the CST following both *Emx1*-Cre-induced deletion and Cre electroporation suggests that the failure of CST at the pyramidal decussation is not due to fate misspecification, which the late ablation using the Cre electroporation would bypass, but instead reveals an intrinsic defect of the tract to project further than the pyramidal decussation in the absence of both *Ldb* proteins.

The defects in the axonal projections of *Ldb1/2*-DKO layer 5 CSMNs led us to investigate whether other subcortical tracts might also be affected by the loss of *Ldb1/2*. To visualize layer 6 corticothalamic projections, we took advantage of the *golli-τ*-EGFP transgene (*golli-EGFP*; Jacobs et al. 2007), in which a *τ*-EGFP cassette, under transcriptional control of 1.3 kb of the *golli* promoter of the myelin basic protein gene, directs EGFP expression to deep layer pyramidal neurons, including layer 6 corticothalamic neurons. In sagittal sections of P4 animals, *golli-EGFP* labeled subcortical efferents, including corticothalamic projections, in both controls and *Ldb2*-KO mice (see Supplementary Fig. 5A,B). Both *Ldb1*-KO (see Supplementary Fig. 5C) and *Ldb1/2*-DKO brains (see Supplementary Fig. 5D) show an obvious reduction in neocortical EGFP expression and reduced corticothalamic innervation (likely due to the reduced number of pyramidal neurons in the mutants), but overall thalamic innervation appears normal in both mutants, suggesting that the formation of corticothalamic projections requires neither *Ldb1* nor *Ldb2*.

Taken together, *Ldb2* is required by layer 5B CSMNs for differentiation and axonal pathfinding into the spinal cord, but the compensatory upregulation of *Ldb1* in *Ldb2<sup>-/-</sup>* mice masks the defects, revealing the requirement for *Ldb2* in the compound *Ldb1/2*-DKO mutants.

### Altered Expression of Axon Guidance Receptors in *Ldb* Mutants

The failure of *Ldb1/2*-DKO CSMN axons to reach the spinal cord and loss of CSMN differentiation markers prompted us to investigate whether axon guidance receptors involved in pathfinding also show altered expression. Neuropilin 1 (*Nrp1*) is a membrane-bound coreceptor for Semaphorins and Plexins, and both *Nrp1* and Semaphorins play roles in axon guidance [reviewed in Huber et al. (2003)]. *Nrp1* expression is detected in layer 5 neurons at P1 in controls and *Ldb2*-KO mice (see Supplementary Fig. 6A,B). In *Ldb1*-KO layer 5 neurons, *Nrp1* expression appears reduced (see Supplementary Fig. 6C,C') and is absent in *Ldb1/2*-DKO animals (although low, diffuse expression over the

cortical wall remains; Supplementary Fig. 6D,D'). No changes in the expression of Semaphorins 3A, 3B, and 3C were found in any of the 4 genotypes for (data not shown).

We then asked whether Eph receptors [reviewed in Flanagan (2006)] showed changes in expression across the 4 genotypes. No changes were found for *EphA3*, *A5*, *A7*, *B1*, and *B2* (data not shown). *EphA4* is expressed by layer 5 neurons and a subset of upper layer neurons at P1; its expression is maintained in *Ldb1*-KO and *Ldb2*-KO mice, but qualitatively reduced in layer 5 of *Ldb1/2*-DKO animals (data not shown). *EphA6* is strongly expressed by layer 5 neurons at P1 (see Supplementary Fig. 6E,E'). Expression is maintained in single mutants (see Supplementary Fig. 6F,G'), but abolished in layer 5 motor cortex of *Ldb1/2*-DKO animals (see Supplementary Fig. 6H,H'). *EphA6* knockout animals suffer from learning and memory impairments (Savelieva et al. 2008), but changes in CST formation have not been reported.

These data indicate that *Ldb1/2* regulates the expression of *Nrp1*, *EphA6*, and *EphA4*. Since several Eph receptors and their ligands have been implicated in defects in CST formation [reviewed in Cauty and Murphy (2008)], it is conceivable that *EphA6* and/or *EphA4* are involved in the defects at the pyramidal decussation of *Ldb1/2*-DKO animals.

## Discussion

We describe a novel involvement of the Lim domain-binding proteins *Ldb1* and *Ldb2* during the development of CSMNs. We find that *Ldb1* and *Ldb2* show inversely correlated expression patterns during cortical development, with a striking localization of *Ldb2* to layer 5 and a concomitant exclusion of *Ldb1* from that layer. Loss of *Ldb1* leads to defects in progenitor proliferation and regionalization. *Ldb2* is required during 2 discrete phases of layer 5 neuron differentiation. It first plays a role during segregation of immature layer 5 neurons into CPNs and SCPNs, resulting in increased fractions of *Ctip2<sup>+</sup>/Lmo4<sup>+</sup>* and *Ctip2<sup>+</sup>/Satb2<sup>+</sup>* double-positive neurons in *Ldb2*-KO layer 5. Second, *Ldb2* is required for differentiation and pathfinding of CSMNs. *Ldb1* is able to compensate for the loss of *Ldb2* for both CSMN differentiation and pathfinding, thus permitting axons to reach the spinal cord in the *Ldb2* single knockout, ultimately revealing the phenotype in compound *Ldb1/2* double knockouts, in which CSMNs fail to extend their axons past the pyramidal decussation due to incomplete molecular differentiation.

### Complex Roles of *Ldb* Proteins Due to Interactions with Multiple Binding Partners

*Ldb* proteins can interact with Lim-HD and Lmo proteins through their Lim-interacting domain. Specific roles for *Ldb* proteins in the brain have not been described yet, but indirect evidence suggests their involvement. For example, the proliferation defects in *Lhx2*-deficient brains and the associated hypoplasia of the neocortex (Porter et al. 1997) correspond well with the proliferation defects we observe in *Ldb1*-KO brains. Given that *Ldb1* strongly binds to *Lhx2* (Agulnick et al. 1996), it is plausible that *Ldb1* functions as an essential cofactor for *Lhx2* function during early stages of cortical development. In support of this model, we observe a regionalization fate change in *Ldb1*-deficient brains, which leads to a shift of piriform cortex into lateral neocortex, concomitant with the appearance of piriform cortex markers in dorsal neocortex. These findings are reminiscent of the changes in regionalization described in a conditional *Lhx2* knockout (Chou et al. 2009), further supporting the notion that *Lhx2* function

requires Ldb1. Intriguingly, the changes in regionalization observed in the Ldb1-KO and Ldb1/2-DKO mice are less pronounced than those observed in the *Lhx2* knockout, suggesting that *Lhx2* signaling could be mediated, at least in part, independently of Ldb1.

### Inversely Correlated Expression Patterns and Compensatory Role of Ldb1 in *Ldb2*<sup>-/-</sup> Mutants

Our analysis reveals a novel, progressive exclusion of *Ldb1* from layer 5 neurons as they begin to express *Ldb2* during differentiation. The inverse correlation between the expression patterns of the 2 family members suggests a regulatory feedback loop that governs the expression of the 2 proteins. It is tempting to speculate that the upregulation of *Ldb2* suppresses the expression of *Ldb1* in layer 5 neurons. Indeed, our data confirm this hypothesis: In *Ldb2*-deficient mutants, we find a striking upregulation of *Ldb1* in layer 5 neurons, suggesting a compensatory role of *Ldb1* in *Ldb2*-KO animals. The expression of *Ldb2* in layer 5 neurons and the concomitant suppression of *Ldb1* suggest that the selective presence of *Ldb2* could act as a switch for differentiation of CSMNs, similar to the combinatorial code involving *Ldb1*, *Lhx3*, and *Isl1* in the spinal cord, where *Ldb1*-*Lhx3* interaction triggers V2 interneuron differentiation, while motor neurons are generated upon *Ldb1*-*Isl1* binding (displacing *Lhx3*; Thaler et al. 2002). The major binding partners for Ldb proteins in the developing cortex include *Lmo3*, *Lmo4*, and *Lhx2*, all of which are expressed in the cortical plate between E15.5 and P3. It is conceivable that the switch from *Ldb1* to *Ldb2* rearranges the interacting protein complexes, in a cell type-specific manner, and consequently changes the differentiation path.

### Impaired Segregation of Layer 5 CPNs and Subcerebral PNs in *Ldb2*-Deficient Brains

The failure in segregation of early layer 5 neurons in *Ldb2*-KO mutants supports the model of a rearrangement of protein interactions by changes in Ldb expression patterns: *Lmo4* is widely coexpressed with *Ctip2* and *Ldb2* in immature layer 5 neurons at E15.5 (Azim et al. 2009). As cortical development proceeds, these layer 5 neurons begin to differentiate into either CPNs or SCPNs, and eventually 2 distinct populations emerge. CPNs downregulate *Ctip2* and *Ldb2*, but maintain expression of *Ldb1*, *Lmo4*, and *Satb2*. SCPNs instead maintain *Ctip2* and *Ldb2*, while downregulating *Ldb1*, *Lmo4*, and *Satb2*. It is tempting to speculate that the suppression of *Ldb1* in layer 5 neurons thus initiates a switch in these cells to acquire a subcerebral (SCPN) fate. In agreement with this model, in *Ldb2*-KO animals, increased fractions of layer 5 neurons coexpressing *Lmo4*/*Ctip2* and *Satb2*/*Ctip2* are found, suggesting that these neurons fail to differentiate properly into either CPNs or SCPNs in the absence of *Ldb2*.

### Incomplete Differentiation of SCPNs in *Ldb* Mutant Mice

Recent evidence suggests that specification and differentiation are comprised of a series of functionally distinct steps: The transcription factor *Fezf2* is required by layer 5 CSMNs for specification, and *Fezf2* knockout animals lack a CST and the majority of CSMN differentiation factors (Chen B et al. 2005; Molyneaux et al. 2005). In contrast, although mice lacking the transcription factor *Bhlhb5* also display defects in the CST, their layer 5 CSMNs appear largely correctly specified, but fail to properly differentiate (Joshi et al. 2008). The expression of both *Ctip2* and

*Fezf2* in *Ldb1/2*-DKO layer 5 neurons indicates that CSMNs are correctly specified in the absence of *Ldb1* and *Ldb2*. However, numerous markers of CSMN differentiation, including *Diap3*, *Foxo1*, *Foxp2*, and *Igf1bp4*, are absent in *Ldb1/2*-DKO brains, representing a significant fraction of the markers lost in *Fezf2* mutants. These data suggest that while initial specification of CSMNs appears unaffected by the loss of *Ldb1* and *Ldb2*, differentiation of CSMNs is incomplete.

The defect in the CST of *Ldb1/2*-DKO animals is surprisingly similar to the defect described in *Bhlhb5*<sup>-/-</sup> mice; axons in both mutant strains fail to extend past the pyramidal decussation, and both strains show loss of some differentiation factors. The pyramidal decussation is a major crossing point for the CST, where the majority of axons cross from the ventral hindbrain to the ventral dorsal funiculus in the spinal cord. It is conceivable that this crossing represents a vulnerable point along the axons' trajectories, and thus is highly susceptible to changes in axon guidance receptor expression. Indeed, our data reveal alterations in the expression of several axon guidance receptors, including *EphA6*, *EphA4*, and *Nrp1*. It is conceivable that the loss of several axon guidance receptors could lead to a failure of axon crossing and extension at the pyramidal decussation.

Taken together, our data suggest a hierarchical relationship between the different stages of pyramidal neuron specification and differentiation: While *Fezf2* is required early for initial CSMN specification, *Ldb2* plays an essential role during late differentiation, perhaps through the rearrangement of protein complexes, when CSMNs extend their axons and refine their identity. Further unraveling of the genetic program that governs differentiation of CSMNs will have pivotal clinical implications for the development of cell replacement therapies for spinal cord injuries and neurodegenerative disorders.

### Supplementary Material

Supplementary material can be found at: <http://www.cercor.oxfordjournals.org/>.

### Funding

This work was supported by the National Institutes of Health (MH051864) to S.K.M.

### Notes

We are grateful to Dr Paul Love for providing anti-Ldb1 antibody. We thank Dr James Weimann for technical help with retrograde injections, Dr Simon Hippenmeyer for helpful suggestions on the manuscript, Elizabeth Alcamo and Alan Agulnick for previous experiments, and Dr Chris Kaznowski for technical help. *Conflict of Interest*: None declared.

### References

- Agulnick AD, Taira M, Breen JJ, Tanaka T, Dawid IB, Westphal H. 1996. Interactions of the LIM-domain-binding factor Ldb1 with LIM homeodomain proteins. *Nature*. 384:270–272.
- Alcamo EA, Chirivella L, Dautzenberg M, Dobрева G, Fariñas I, Grosschedl R, McConnell SK. 2008. *Satb2* regulates callosal projection neuron identity in the developing cerebral cortex. *Neuron*. 57:364–377.
- Arlotta P, Molyneaux BJ, Chen J, Inoue J, Kominami R, Macklis JD. 2005. Neuronal subtype-specific genes that control corticospinal motor neuron development in vivo. *Neuron*. 45:207–221.

- Arlotta P, Molyneaux BJ, Jabaudon D, Yoshida Y, Macklis JD. 2008. *Tip2* controls the differentiation of medium spiny neurons and the establishment of the cellular architecture of the striatum. *J Neurosci*. 28:622–632.
- Asprer JS, Lee B, Wu CS, Vadakkan T, Dickinson ME, Lu HC, Lee SK. 2011. LMO4 functions as a co-activator of neurogenin 2 in the developing cortex. *Development*. 138:2823–2832.
- Azim E, Shnyder SJ, Cederquist GY, Sohur US, Macklis JD. 2009. Lmo4 and Clim1 progressively delineate cortical projection neuron subtypes during development. *Cereb Cortex*. 19 (Suppl 1):i62–i69.
- Bach I, Carrière C, Ostendorff HP, Andersen B, Rosenfeld MG. 1997. A family of LIM domain-associated cofactors confer transcriptional synergism between LIM and Otx homeodomain proteins. *Genes Dev*. 11:1370–1380.
- Breen JJ, Agulnick AD, Westphal H, Dawid IB. 1998. Interactions between LIM domains and the LIM domain-binding protein Ldb1. *J Biol Chem*. 273:4712–4717.
- Britanova O, de Juan Romero C, Cheung A, Kwan KY, Schwark M, Gyorgy A, Vogel T, Akopov S, Mitkovski M, Agoston D, et al. 2008. *Satb2* is a postmitotic determinant for upper-layer neuron specification in the neocortex. *Neuron*. 57:378–392.
- Bulchand S, Subramanian L, Tole S. 2003. Dynamic spatiotemporal expression of LIM genes and cofactors in the embryonic and postnatal cerebral cortex. *Dev Dyn*. 226:460–469.
- Canty AJ, Murphy M. 2008. Molecular mechanisms of axon guidance in the developing corticospinal tract. *Prog Neurobiol*. 85:214–235.
- Chen B, Schaevitz LR, McConnell SK. 2005. *Fez1* regulates the differentiation and axon targeting of layer 5 subcortical projection neurons in cerebral cortex. *Proc Natl Acad Sci USA*. 102:17184–17189.
- Chen JG, Rasin MR, Kwan KY, Sestan N. 2005. *Zfp312* is required for subcortical axonal projections and dendritic morphology of deep-layer pyramidal neurons of the cerebral cortex. *Proc Natl Acad Sci USA*. 102:17792–17797.
- Chou SJ, Perez-Garcia CG, Kroll TT, O'Leary DD. 2009. *Lhx2* specifies regional fate in *Emx1* lineage of telencephalic progenitors generating cerebral cortex. *Nat Neurosci*. 12:1381–1389.
- Englund C, Fink A, Lau C, Pham D, Daza RA, Bulfone A, Kowalczyk T, Hevner RF. 2005. *Pax6*, *Tbr2*, and *Tbr1* are expressed sequentially by radial glia, intermediate progenitor cells, and postmitotic neurons in developing neocortex. *J Neurosci*. 25:247–251.
- Flanagan JG. 2006. Neural map specification by gradients. *Curr Opin Neurobiol*. 16:59–66.
- Frantz GD, Weimann JM, Levin ME, McConnell SK. 1994. *Otx1* and *Otx2* define layers and regions in developing cerebral cortex and cerebellum. *J Neurosci*. 14:5725–5740.
- Gorski JA, Talley T, Qiu M, Puellas L, Rubenstein JL, Jones KR. 2002. Cortical excitatory neurons and glia, but not GABAergic neurons, are produced in the *Emx1*-expressing lineage. *J Neurosci*. 22:6309–6314.
- Han W, Kwan KY, Shim S, Lam MM, Shin Y, Xu X, Zhu Y, Li M, Sestan N. 2011. *TBR1* directly represses *Fezf2* to control the laminar origin and development of the corticospinal tract. *Proc Natl Acad Sci USA*. 108:3041–3046.
- Hevner RF, Shi L, Justice N, Hsueh Y, Sheng M, Smiga S, Bulfone A, Goffinet AM, Campagnoni AT, Rubenstein JL. 2001. *Tbr1* regulates differentiation of the preplate and layer 6. *Neuron*. 29:353–366.
- Huang Z, Kawase-Koga Y, Zhang S, Visvader J, Toth M, Walsh CA, Sun T. 2009. Transcription factor *Lmo4* defines the shape of functional areas in developing cortices and regulates sensorimotor control. *Dev Biol*. 327:132–142.
- Huber AB, Kolodkin AL, Ginty DD, Cloutier JF. 2003. Signaling at the growth cone: ligand-receptor complexes and the control of axon growth and guidance. *Annu Rev Neurosci*. 26:509–563.
- Jacobs EC, Campagnoni C, Kampf K, Reyes SD, Kalra V, Handley V, Xie YY, Hong-Hu Y, Spreur V, Fisher RS, et al. 2007. Visualization of corticofugal projections during early cortical development in a tau-GFP-transgenic mouse. *Eur J Neurosci*. 25:17–30.
- Jones EG, Schreyer DJ, Wise SP. 1982. Growth and maturation of the rat corticospinal tract. *Prog Brain Res*. 57:361–379.
- Joshi PS, Molyneaux BJ, Feng L, Xie X, Macklis JD, Gan L. 2008. *Bhlhb5* regulates the postmitotic acquisition of area identities in layers II–V of the developing neocortex. *Neuron*. 60:258–272.
- Jurata LW, Gill GN. 1997. Functional analysis of the nuclear LIM domain interactor NLI. *Mol Cell Biol*. 17:5688–5698.
- Jurata LW, Kenny DA, Gill GN. 1996. Nuclear LIM interactor, a rhombotin and LIM homeodomain interacting protein, is expressed early in neuronal development. *Proc Natl Acad Sci USA*. 93:11693–11698.
- Kenny DA, Jurata LW, Saga Y, Gill GN. 1998. Identification and characterization of LMO4, an LMO gene with a novel pattern of expression during embryogenesis. *Proc Natl Acad Sci USA*. 95:11257–11262.
- Kwan KY, Lam MM, Krsnik Z, Kawasaki YI, Lefebvre V, Sestan N. 2008. *SOX5* postmitotically regulates migration, postmigratory differentiation, and projections of subplate and deep-layer neocortical neurons. *Proc Natl Acad Sci USA*. 105:16021–16026.
- Lee SK, Jurata LW, Nowak R, Lettieri K, Kenny DA, Pfaff SL, Gill GN. 2005. The LIM domain-only protein LMO4 is required for neural tube closure. *Mol Cell Neurosci*. 28:205–214.
- Leone DP, Heavner WE, Ferenczi EA, Dobrev G, Huguenard JR, Grosschedl R, McConnell SK. 2015. *Satb2* regulates the differentiation of both callosal and subcerebral projection neurons in the developing cerebral cortex. *Cereb Cortex*. 25:3406–3419.
- Mangale VS, Hirokawa KE, Satyaki PR, Gokulchandran N, Chikbire S, Subramanian L, Shetty AS, Martynoga B, Paul J, Mai MV, et al. 2008. *Lhx2* selector activity specifies cortical identity and suppresses hippocampal organizer fate. *Science*. 319:304–309.
- Matthews JM, Visvader JE. 2003. LIM-domain-binding protein 1: a multifunctional cofactor that interacts with diverse proteins. *EMBO Rep*. 4:1132–1137.
- McKenna WL, Betancourt J, Larkin KA, Abrams B, Guo C, Rubenstein JL, Chen B. 2011. *Tbr1* and *Fezf2* regulate alternate corticofugal neuronal identities during neocortical development. *J Neurosci*. 31:549–564.
- Meier N, Krpic S, Rodriguez P, Strouboulis J, Monti M, Krijgsveld J, Gering M, Patient R, Hostert A, Grosfeld F. 2006. Novel binding partners of Ldb1 are required for haematopoietic development. *Development*. 133:4913–4923.
- Molyneaux BJ, Arlotta P, Hirata T, Hibi M, Macklis JD. 2005. *Fez1* is required for the birth and specification of corticospinal motor neurons. *Neuron*. 47:817–831.
- Mori M, Kose A, Tsujino T, Tanaka C. 1990. Immunocytochemical localization of protein kinase C subspecies in the rat spinal cord: light and electron microscopic study. *J Comp Neurol*. 299:167–177.
- Mukhopadhyay M, Teufel A, Yamashita T, Agulnick AD, Chen L, Downs KM, Schindler A, Grinberg A, Huang SP, Dorward D, et al. 2003. Functional ablation of the mouse *Ldb1* gene results in severe patterning defects during gastrulation. *Development*. 130:495–505.

- Novak A, Guo C, Yang W, Nagy A, Lobe CG. 2000. Z/EG, a double reporter mouse line that expresses enhanced green fluorescent protein upon Cre-mediated excision. *Genesis*. 28:147–155.
- Ohtsuka T, Sakamoto M, Guillemot F, Kageyama R. 2001. Roles of the basic helix-loop-helix genes *Hes1* and *Hes5* in expansion of neural stem cells of the developing brain. *J Biol Chem*. 276:30467–30474.
- Porter FD, Drago J, Xu Y, Cheema SS, Wassif C, Huang SP, Lee E, Grinberg A, Massalas JS, Bodine D, et al. 1997. *Lhx2*, a LIM homeobox gene, is required for eye, forebrain, and definitive erythrocyte development. *Development*. 124:2935–2944.
- Savelieva KV, Rajan I, Baker KB, Vogel P, Jarman W, Allen M, Lanthorn TH. 2008. Learning and memory impairment in Eph receptor A6 knockout mice. *Neurosci Lett*. 438:205–209.
- Shim S, Kwan KY, Li M, Lefebvre V, Sestan N. 2012. Cis-regulatory control of corticospinal system development and evolution. *Nature*. 486:74–79.
- Sugihara TM, Bach I, Kioussi C, Rosenfeld MG, Andersen B. 1998. Mouse deformed epidermal autoregulatory factor 1 recruits a LIM domain factor, LMO-4, and CLIM coregulators. *Proc Natl Acad Sci USA*. 95:15418–15423.
- Thaler JP, Lee SK, Jurata LW, Gill GN, Pfaff SL. 2002. LIM factor *Lhx3* contributes to the specification of motor neuron and interneuron identity through cell-type-specific protein-protein interactions. *Cell*. 110:237–249.
- Tomassy GS, De Leonibus E, Jabaudon D, Lodato S, Alfano C, Mele A, Macklis JD, Studer M. 2010. Area-specific temporal control of corticospinal motor neuron differentiation by COUP-TFI. *Proc Natl Acad Sci USA*. 107:3576–3581.
- Tse E, Smith AJ, Hunt S, Lavenir I, Forster A, Warren AJ, Grutz G, Foroni L, Carlton MB, Colledge WH, et al. 2004. Null mutation of the *Lmo4* gene or a combined null mutation of the *Lmo1/Lmo3* genes causes perinatal lethality, and *Lmo4* controls neural tube development in mice. *Mol Cell Biol*. 24:2063–2073.
- Visvader JE, Mao X, Fujiwara Y, Hahm K, Orkin SH. 1997. The LIM-domain binding protein *Ldb1* and its partner *LMO2* act as negative regulators of erythroid differentiation. *Proc Natl Acad Sci USA*. 94:13707–13712.
- Wadman I, Li J, Bash RO, Forster A, Osada H, Rabbitts TH, Baer R. 1994. Specific *in vivo* association between the bHLH and LIM proteins implicated in human T cell leukemia. *EMBO J*. 13:4831–4839.
- Wadman IA, Osada H, Grütz GG, Agulnick AD, Westphal H, Forster A, Rabbitts TH. 1997. The LIM-only protein *Lmo2* is a bridging molecule assembling an erythroid, DNA-binding complex which includes the *TAL1*, *E47*, *GATA-1* and *Ldb1/NLI* proteins. *EMBO J*. 16:3145–3157.
- Zhao Y, Kwan KM, Mailloux CM, Lee WK, Grinberg A, Wurst W, Behringer RR, Westphal H. 2007. LIM-homeodomain proteins *Lhx1* and *Lhx5*, and their cofactor *Ldb1*, control Purkinje cell differentiation in the developing cerebellum. *Proc Natl Acad Sci USA*. 104:13182–13186.
- Zhao Y, Sheng HZ, Amini R, Grinberg A, Lee E, Huang S, Taira M, Westphal H. 1999. Control of hippocampal morphogenesis and neuronal differentiation by the LIM homeobox gene *Lhx5*. *Science*. 284:1155–1158.